Choked flame and its transition to detonation in an obstructed channel

Jumeng Fan, Min Li, Huahua Xiao*
State Key Laboratory of Fire Science, University of Science and Technology of China
Hefei, Anhui 230027, China

1 Introduction

Choked flames appear in the late stages of flame acceleration and before the onset of detonations at the maximum deflagration speed [1].The properties of choked flames and their eventual transition to detonations are relevant in the study of events such as large-scale explosions, and ignition in detonation-based propulsion and power generation devices. However, the mechanisms of choked flame and the subsequent transition into detonation are much less understood

In terms of the maximum deflagration speed at which the choked flame propagates, which serves as a crucial criterion for the transition to detonation, three primary viewpoints have been proposed. Firstly, it was experimentally verified that the maximum deflagration speed of a choked flame propagating in congested tubes with closed ends was approximately equal to the sound speed in the burned gases [1]. Secondly, Chue et al. [2] presented a simple double discontinuity self-similar model for steady Chapman-Jouguet (CJ) deflagrations that drive a shock ahead of it. The CJ deflagration velocity, related to the choking regime of propagation, has been successfully used as a criterion for the transition to detonation [3, 4]. Thirdly, in subsequent confined experiments where transition was suppressed by gas dynamic quenching, it was confirmed that approximately half the CJ detonation speed agreed very well with the maximum deflagration speed [5, 6]. Conventionally, the sound speed in the burned gases, the CJ deflagration speed, and half the CJ detonation speed are often approximated as equivalent criteria for the transition to detonation. Nevertheless, these parameters not only differ in their fundamental physical mechanisms but also exhibit numerical distinctions. In summary, the mechanisms and crucial conditions that govern choked flames and the transition to detonation within obstructed channels are still ambiguously defined.

The objective of this work is to study the effect of initial pressure and blockage ratio on the choked flame and transition to detonation in an obstructed channel using numerical simulations.

2 Mathematical model and numerical method

The details of numerical method and grid resolution tests were extensively outlined in our prior papers [7, 8]. Hydrogen-oxygen combustion was considered utilizing a calibrated chemical-diffusion model,

Correspondence to: xiaoh@ustc.edu.cn

which has been tested and has been applied to a diverse array of combustion scenarios, such as laminar and turbulent flames [8-10], DDT [11-13], and cellular detonations [12].

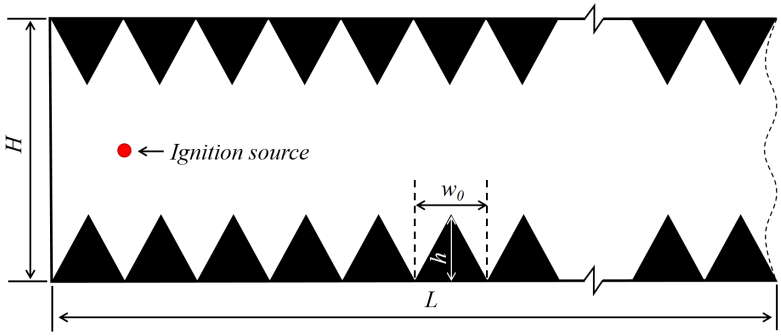

Figure 1: Computational domain of an obstructed channel, referring the experiment by Li et al. [14].

Figure shows the two-dimensional computational domain. The conditions model the experiments by Li et al. [14]. It is an obstructed channel, 0.02 m (H) × 0.3 m (L). Each triangular obstacle is 0.58 cm wide (w_0), which spans the width of the channel. The blockage ratio of the channel is $br = 2h/H$, where h is the obstacle height. A third-order WENO algorithm with HLLC fluxes is used to solve the fully compressible, reactive Navier-Stokes equations on a dynamically adapted mesh. Time integration is done by the explicit second-order explicit Runge-Kutta. No-slip adiabatic boundary conditions are used at the left end wall and obstacle surfaces, and the right end is non-reflecting boundary. The ignition source is a circular region of burned material with a radius of 1 mm. The initial temperature of premixed unburned gases is 298 K.

3 Result and discussion

3.1 Comparison to experiment

Figure 2 compares the experimental and numerical schlieren images of flame acceleration to choked flame and the subsequent transition to detonation for $br = 0.5$, $p_0 = 70$ kPa. The images are selected at specific times when the reaction front tips in the experiment and simulation reach a consistent location. Overall, the evolution of the flame, flow, shock, and detonation wave in the simulation agree well with those observed in the experiment. In the early stages, the laminar flame expands outward, generating a sequence of vortices in the downstream obstacle gaps. As the flame reaches the vortices, the flame is rapidly drawn and entrained into these vortices, as shown in Fig. 2 at 0.15 ms and 0.11 ms in the experiment and simulation, respectively. In the later stages, the flame develops significantly corrugated and intensifies its acceleration, leading to the generation of compression waves ahead of it. The merging of these compression waves results in the formation of a leading shock. This leading shock continuously amplifies, and the distance between the reaction front and the leading shock (d_{s-f}) shortens as the flame accelerates, until forming a choked flame. The change of d_{s-f} is consistent with that observed in the experiment, as shown in Fig. 2 at 0.22 and 0.26 ms in the experiment, 0.18 and 0.23 ms in the simulation in Fig. 2. After the flame propagating through a choking regime for a period of time, detonation is initiated and continues to sweep across the channel. Figure 3 compares the calculated, experimental, and theoretical results in the early stage of flame acceleration. The results show that Bychkov theory gives a reasonable prediction of the speed of the flame tip, when $br = 0.5$.

The qualitative and quantitative agreement with the experiments and Bychkov theory [15] confirms the validity of the numerical simulation for exploring the mechanisms of FA, choked flame, and DDT.

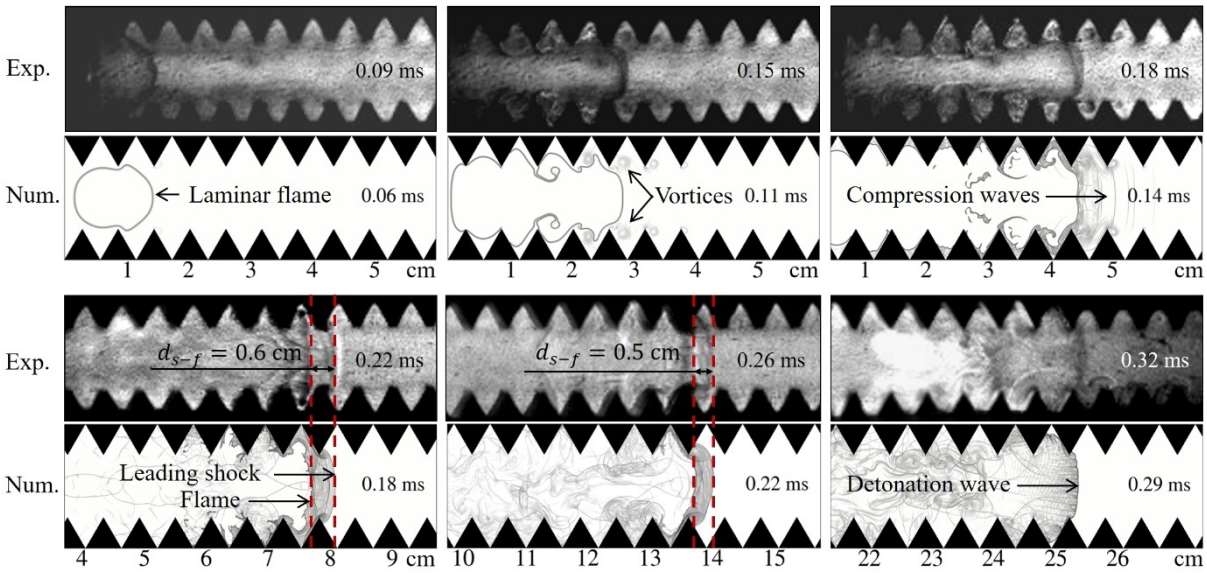

Figure 2: Comparison between experimental and numerical schlieren images of flame acceleration to choked flame and detonation transition for br = 0.5, p_0 = 70 kPa.

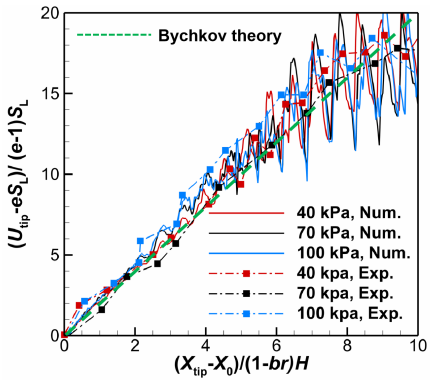

Figure 3: Comparison between numerical simulation and Bychkov theory [15] regarding the scaled speed of the flame tip versus the scaled tip position, br = 0.5 at different initial pressures.

3.2 Effect of pressure

Figure 4 shows the reaction front speed and area as a function of position for br = 0.5 at different initial pressures. To display the stage of the choked flame more clearly, the reaction front speed after DDT is not depicted here. Fig. 5 shows the temperature fields of the flame acceleration to choked state and transition to detonation for various initial pressures of (a) 40 kPa, (b) 70 kPa, and (c) 100 kPa. The fields are selected at specific times when the reaction front tips in the three cases reach a consistent location. Figures 4 and 5 show that before flame accelerates to CJ deflagration speed (S_{CJ}), the flame development process under the three pressure conditions is largely consistent, aligning with the description in Section 3.1. However, as the flame reaches a comparable position, the flame exhibits a greater degree of curling at higher initial pressures (see Fig. 5 (2)), the generation of the compression wave occurs earlier (see Fig. 5 (3)), and the shock wave is stronger (as see Fig. 5 (4)). Particularly after the flame accelerates to S_{CJ}, significant differences in the propagation mechanism become apparent.

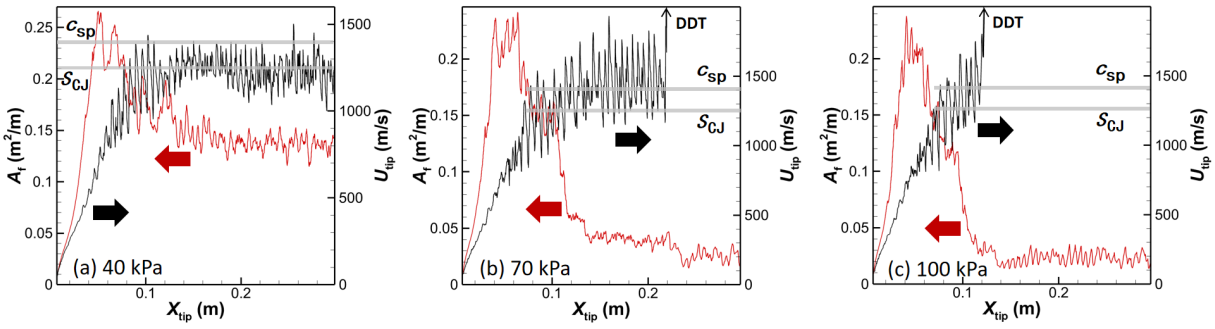

Figure 4: The reaction front speed (U_{tip}) and area (A_f) as a function of position (x_{tip}) for $br = 0.5$ at an initial pressure of (a) 40 kPa, (b)70 kPa, and (c) 100 kPa.

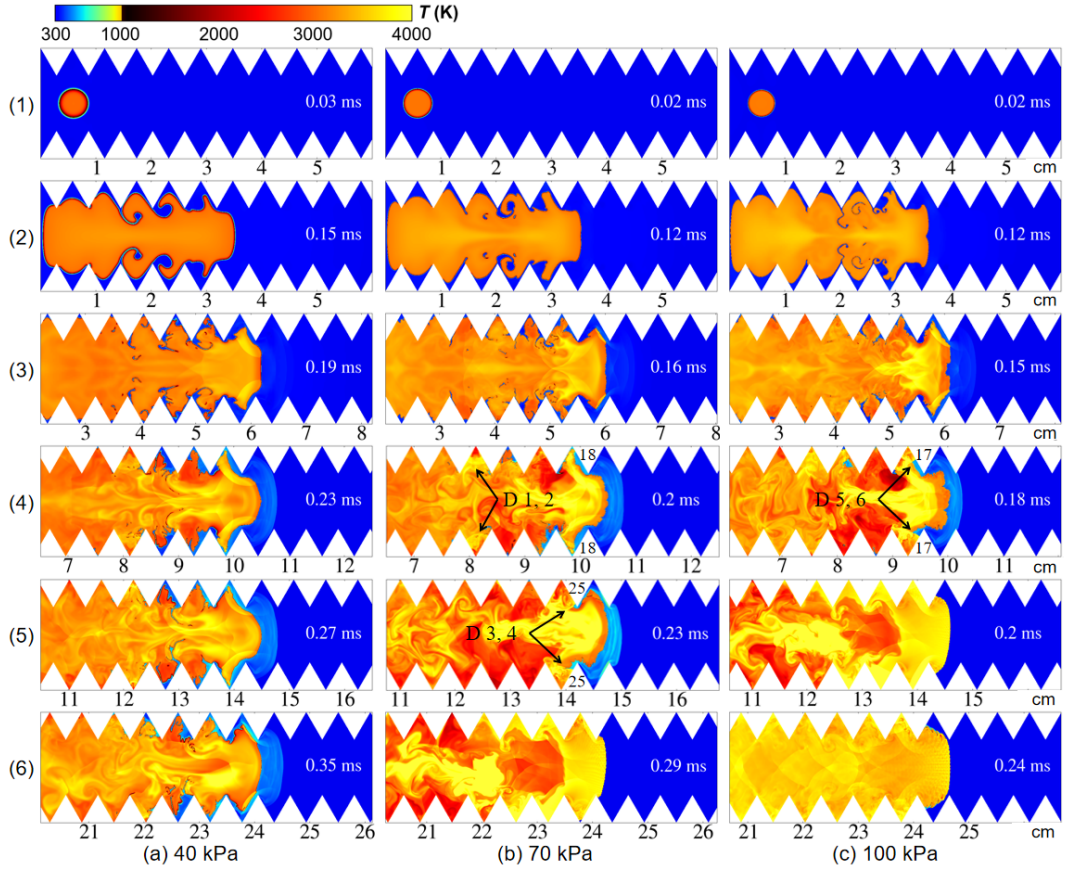

Figure 5: Sequences of numerical temperature maps showing the flame acceleration to choked state and detonation transition for various initial pressures of (a) 40 kPa, (b) 70 kPa, and (c) 100 kPa.

For an initial pressure of 40 kPa, the flame propagates forward in a choked state after accelerating to S_{CJ} until reaching the end of the channel. The average choked velocity consistently aligns with S_{CJ}. Throughout the process of choked flame propagation, no local explosions occur. The distance between the rear end of the flame skirt and the flame tip is maintained at approximately 3-4 obstacles (e.g., Fig. 5a), correlating with the larger flame area shown in Fig. 4a. For an initial pressure of 70 kPa, once the flame crosses the 18th obstacle (approximately x_{tip} = 10 cm), the flame propagation speed reaches S_{CJ} (see Fig. 4b), and the first pair of local explosions, D1 and D2, occur (see Fig. 5b at 0.2 ms). These local explosions rapidly consume the unburned gas within the gaps between the obstacles, resulting in a sharp reduction in flame area (Fig. 4b at 0.1 m). Subsequently, the flame continues to accelerate and remains

choked at a velocity of the sound speed in the burned gases (c_{sp}). Local explosions occur in the intervals between each obstacle (e.g., at 0.23 ms, D 3 and D 4 in Fig. 5). After the choking state lasting about 10 cm, detonation is successfully initiated, evident through a sudden surge in reaction front velocity and a second abrupt decrease in flame area, reducing to the height of the channel (Fig. 4b at 0.22 ms). For an initial pressure of 100kPa, after the flame crossed the 17th obstacle (about x_{tip} = 10cm), the flame velocity reached S_{CJ} (Fig. 4c), and the first pair of local explosions D 5, 6 occurs (Fig. 5c at 0.18ms), which is like the case at 70kPa. Differently, at 100kPa, following the flame acceleration to c_{sp}, choking does not take place, instead, DDT occurs directly. This detonation was marked by a sudden surge in reaction front velocity and an immediate decrease in flame area to the height of the channel (see Fig. 4c).

3.3 Effect of blockage ratio

Figure 6 shows the reaction front speed and area as a function of position at an initial pressure 70 kPa for different blockage ratios. The results show that while the early flame acceleration process is influenced by the blockage ratio, flames across all blockage ratios achieve acceleration to the maximum possible deflagration speed, S_{CJ} = 1270 m/s. After accelerating to S_{CJ}, the propagation pattern of combustion waves shows notable variations based on the blockage ratios. While the case of an intermediate blockage ratio, br = 0.5, was discussed in section 4.1, the focus now shifts to discussing br = 0.3 and br = 0.7.

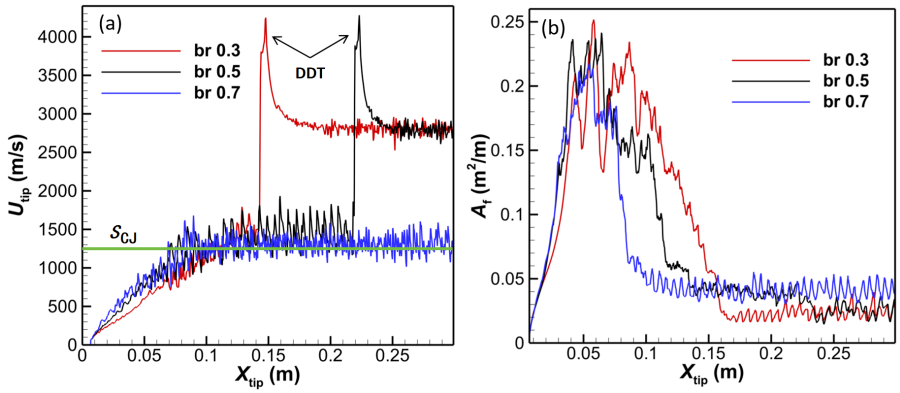

Figure 6: (a) The reaction front speed (U_{tip}) and (b) reaction front area (A_f) as a function of position (x_{tip}) at an initial pressure 70 kPa for different blockage ratios.

In channels with higher blockage ratios, flames exhibit faster early acceleration due to the larger flame area, and the attenuation of flame acceleration in the later stage is more pronounced due to the influence of stronger reflected shock waves. Nevertheless, all low, medium, and high blockage ratios facilitate the flame acceleration to S_{CJ} and the generation of localized explosions. It is noteworthy that higher blockage ratio leads to earlier local explosions, yet these local explosions face greater challenges in progressing beyond the flame front to achieve detonation.

4 Conclusions

Experiments and numerical simulations were conducted in this study to explore choked flame phenomena and the transition to detonation in an obstructed channel. Different initial pressures (40, 70, and 100 kPa) at a fixed blockage ratio of 0.5 and various blockage ratios (0.3, 0.5, and 0.7) at a fixed initial pressure of 70 kPa were considered. The experiments used high-speed photography to record the propagation of the combustion wave. The 2D fully compressible reactive Navier-Stokes equations,

coupled with a calibrated chemical-diffusive model, were solved using a third-order WENO algorithm on a locally adapting grid.

The results indicate that the simulations align well with the experiments and Bychkov theory for all the initial pressures considered. Once the flame accelerates to the CJ deflagration speed, the flame propagation pattern is categorized into three groups: completely choked flame, choked flame to detonation transition, and DDT directly without choking stage. A decrease in pressure or an increase in blockage ratio can alter the flame propagation pattern from DDT directly to complete choking. The completely choked flame propagats at the CJ deflagration speed. However, noticeable differences exist in the choking regime between decreasing the pressure and increasing the blockage ratio.

As pressure decreases, the detonation stability of the mixture decreases. In the same channel configuration (i.e., with consistent shock reflection and convergence), mixtures with low detonation stability face greater challenges in generating local hot spots under CJ deflagration conditions. Consequently, reduced pressure leads to a completely choked flame with minimal local hot spot generation during propagation. On the other hand, as the blockage ratio increases, the space between the bulk flame and the obstacle vertex diminishes. With the same pressure (i.e., equivalent ability to generate local hot spots), the narrower diffraction space makes it tougher for local detonation in the obstacle gaps to survive. Thus, higher blockage ratios make it easier for the flame to remain choked and harder for detonation initiation to take place.

References

[1] Lee JH, Knystautas R, Chan CK, (1984) Turbulent flame propagation in obstacle-filled tubes, The Combustion Institute.
[2] Chue RS, Clarke JF, Lee JH, (1993) Chapman-Jouguet deflagrations, P Roy Soc 441: 607-623.
[3] Saif M, Wang WT, Pekalski A, Levin M, Radulescu MI, (2017) Chapman-Jouguet deflagrations and their transition to detonation, Proc. Combust. Inst. 36: 2771-2779.
[4] Poludnenko AY, Gardiner TA, Oran ES, (2011) Spontaneous transition of turbulent flames to detonations in unconfined media, Phys. Rev. Lett. 107.
[5] Ciccarelli G, Dorofeev S, (2008) Flame acceleration and transition to detonation in ducts, Prog. Energy Combust. Sci. 34: 499-550.
[6] Mehr SH, Ciccarelli G, (2023) DDT run-up distance in an obstructed tube, Combust. Flame 255.
[7] Fan J, Li M, Xiao H, (2024) Effect of composition gradient on detonation initiation in fuel-rich hydrogen-air mixtures in an obstructed channel, Int. J. Hydrog. Energy 72: 976-990.
[8] Fan J, Xiao H, (2022) Flame acceleration and transition to detonation in non-uniform hydrogen-air mixtures in an obstructed channel with different obstacle arrangements, Fire. Saf. J. 133: 103660.
[9] Xiao H, Houim RW, Oran ES, (2017) Effects of pressure waves on the stability of flames propagating in tubes, Proc. Combust. Inst. 36: 1577-1583.
[10] Poludnenko AY, Oran ES, (2010) The interaction of high-speed turbulence with flames: Global properties and internal flame structure, Combust. Flame 157: 995-1011.
[11] Gamezo VN, Ogawa T, Oran ES, (2007) Numerical simulations of flame propagation and DDT in obstructed channels filled with hydrogen-air mixture, Proc. Combust. Inst. 31: 2463-2471.
[12] Kessler DA, Gamezo VN, Oran ES, (2011) Multilevel detonation cell structures in methane-air mixtures, Proc. Combust. Inst. 33: 2211-2218.
[13] Xiao H, Oran ES, (2019) Shock focusing and detonation initiation at a flame front, Combust. Flame 203: 397-406.
[14] Li X, Dong J, Jin K, Duan Q, Sun J, Li M, Xiao H, (2022) Flame acceleration and deflagration-to-detonation transition in a channel with continuous triangular obstacles: Effect of equivalence ratio, Process Saf. Environ. Prot. 167: 576-591.
[15] Bychkov V, Valiev D, Eriksson LE, (2008) Physical mechanism of ultrafast flame acceleration, PRL 101.